Acta Mech 222, 233–244 (2011)
DOI 10.1007/s00707-011-0537-4

L. W. Guo · J. L. Yu

Bending behavior of aluminum foam-filled double cylindrical tubes

Received: 3 December 2010 / Published online: 7 August 2011

Abstract Quasi-static experiments and numerical simulations are carried out to study three-point bending behavior of a new kind of structures, i.e., double cylindrical tubes filled with closed-cell aluminum foam. The deformation and failure mechanism of this new structure were observed and analyzed numerically using the finite element method. It is revealed that the stress distribution and fracture of the foam-filled double-tube structure are different from those of an empty tube and foam-filled single tube. Two cracks were found experimentally, and both experiments and numerical simulation show that cracks initiated in the aluminum foam. In comparison with empty and foam-filled single tubes, the load-carrying capacity of this new structure is much steadier, the bending resistance is enhanced, and the weight efficiency of energy absorption is higher. Parameters affecting the performance of the foam-filled double-tube structures are also studied.

1 Introduction

During the past two decades, many research works have been done to study the axial crushing behavior of thin-walled columns, which work as energy absorption members, in order to improve their capacity [1–3]. On the other hand, a study on the real-world vehicle crashes showed that up to 90% involved structural members failed in bending collapse mode [4].

As the results obtained in many related works, empty tubes are not suitable for bearing three-point bending loads due to their very low resistance to indentation. In order to achieve higher bending resistance and weight efficiency in energy absorption, ultra-light metal fillers such as aluminum foams were filled into thin-walled structures. The bending behavior of such structures was studied by many researchers in the past several years. Santosa and Wierzbicki [5] and Santosa et al. [6] investigated the effect of foam filling on the bending resistance of thin-walled square columns through numerical simulation and quasi-static experiments. It was shown that filling of foam improved the load-carrying capacity by offering additional support from inside and increases the energy absorption. It was also pointed out that partial filling of foams increased the energy absorption to weight ratio of the structure. The three-point bending behavior of the foam-filled cylindrical tubes was studied by Xie et al. [7,8]. They showed that higher foam density could increase the load-carrying capacity of the foam-filled cylindrical tube but will reduce the displacement before failure. The bending behavior of hat profiles filled with

L. W. Guo · J. L. Yu (✉)
CAS Key Laboratory of Mechanical Behavior and Design of Materials,
University of Science and Technology of China, Hefei 230027, Anhui, People's Republic of China
E-mail: jlyu@ustc.edu.cn
Tel.: +86-551-360-0792
Fax: +86-551-360-6459

L. W. Guo
Science and Technology on Shock Waves and Detonation Physics Laboratory,
Institute of Fluid Physics, CAEP, Mianyang 621900, Sichuan, People's Republic of China

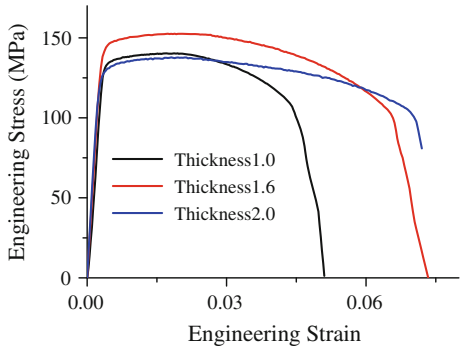

Fig. 1 Engineering stress–strain curves of the profile materials

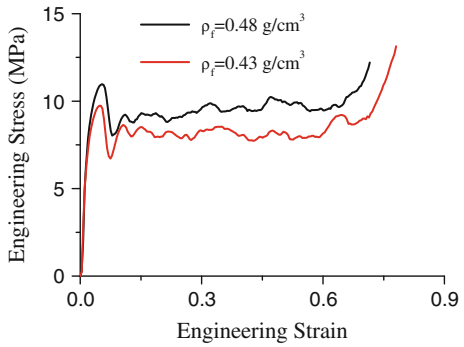

Fig. 2 Uniaxial compression stress–strain curves of aluminum foams

aluminum foams was studied by Chen [9]. It was found that filling of aluminum foams increased the specific energy absorption of the structures. Chen et al. [10] performed numerical simulation and weight optimization on foam-filled sections under bending condition. The results showed the potential of thin-walled columns filled with aluminum foams as weight-efficient energy absorbers. Zarei and Kröger [11] studied the bending crash behavior of empty and foam-filled thin-walled square aluminum beams experimentally and numerically. An optimization procedure was applied to find the optimum foam-filled beam that absorbs the same energy as optimum empty tubes with lower weight. Kim et al. [12] studied the bending collapse of thin-walled cylindrical tubes filled with several pieces of foams experimentally and numerically. They pointed out that the bending resistance of tubes with three pieces of filler was higher than that with one piece of filler.

For a structure under bending, the energy absorption as well as the bending resistance is of importance when considering its crashworthiness. Although filling of aluminum foams increases the bending resistance of thin-walled columns, it is found that columns filled with aluminum foams fail much earlier than those without fillers, which limits the energy absorption of the structures. In this paper, the quasi-static three-point bending behavior of an improved structure, i.e., double cylindrical tubes filled with closed-cell aluminum foam, is studied in detail experimentally and numerically. The deformation and failure mechanism are analyzed, and the results are compared with those of empty tubes and foam-filled single tubes.

2 Experimental setup

2.1 Specimens

The tube material used in the experiments is AA 6063 T6. Uniaxial tension test results of the material are shown in Fig. 1. Slight differences for material AA 6063 T6 with different thicknesses were found. The closed-cell aluminum foam was provided by Luoyang Ship Material Institute, CSIC, China, and produced by liquid state processing using TiH_2 as foaming agent. The uniaxial compression test results of the foams are shown in Fig. 2 where ρ_f denotes the apparent density of the foam.

Table 1 Dimensions of cylindrical tubes (in mm)

	Outer tube		Inner tube	
	Diameter (mm)	Thickness (mm)	Diameter (mm)	Thickness (mm)
1	38	1.0	20	1.2
2	38	1.6	24	1.2
3	38	2.0	22	1.4

Table 2 The parameters of specimens

Specimen	Profiles (outer-inner)		Aluminum foams		m_t (g)	S_{max} (mm)	E_{max} (J)	E_s (J/g)
	Thickness (mm)	Mass (g)	Mass (g)	Density (g/cm^3)				
6E20a	1.6–0	124.5–0	–	–	124.5	–	–	–
6E20b	1.6–0	124.5–0	–	–	124.5	–	–	–
6S20a	1.6–0	124.5–0	114.0	0.44	238.5	12.9	55.9	0.23
6S20b	1.6–0	124.5–0	124.2	0.48	248.7	11.2	49.2	0.20
6D21a	1.6–1.2	124.5–42.4	81.0	0.47	247.9	26.3	111.3	0.45
6D21b	1.6–1.2	124.5–42.4	79.1	0.46	246.0	27.6	115.3	0.47
6D11a	1.0–1.2	83.0–42.3	95.0	0.50	220.3	17.2	56.0	0.25
6D11b	1.0–1.2	82.9–42.3	92.6	0.49	217.8	18.9	62.8	0.29
6D31a	2.0–1.2	152.8–42.3	84.6	0.53	279.7	42.5	212.0	0.76
6D31b	2.0–1.2	153.0–42.3	86.2	0.54	281.5	28.0	142.0	0.50
6D22a	1.6–1.2	124.5–51.6	73.3	0.54	249.4	40.3	155.6	0.62
6D22b	1.6–1.2	124.5–51.6	70.2	0.52	246.3	43.1	164.1	0.67
6D23a	1.6–1.4	124.5–59.6	85.8	0.56	269.9	26.2	141.2	0.52
6D23b	1.6–1.4	124.5–59.6	84.8	0.55	268.9	26.4	144.0	0.54
4E20a	1.6–0	87.5–0	–	–	87.5	–	–	–
4E20b	1.6–0	87.5–0	–	–	87.5	–	–	–
4S20a	1.6–0	87.5–0	76.8	0.42	164.3	13.3	70.9	0.43
4S20b	1.6–0	87.5–0	84.7	0.47	172.2	10.6	55.8	0.32
4D21a	1.6–1.2	87.5–29.8	55.5	0.46	172.8	26.4	140.3	0.81
4D21b	1.6–1.2	87.5–29.8	60.1	0.50	117.3	24.0	138.5	1.20

Empty tube Single tube with foam Double tube with foam

Fig. 3 Sections of different tube arrangements

Table 1 gives the dimensions of the cylindrical tubes in the experiments. The parameters of specimens are listed in Table 2. The specimens in this paper are named according to the following rule. The first number in the specimen named "6D21a" means the ratio of the span L_0 to the diameter D of the outer tube, followed by the arrangement or filling status that E means empty tubes, S means foam-filled single tubes, and D means foam-filled double tubes. The third and fourth number means the type of outer and inner tube, respectively, in Table 1. The last letter is a serial number of each specimen type. The arrangements of different structures are shown in Fig. 3.

2.2 Experimental details

The arrangement of the three-point bending is shown in Fig. 4. MTS809 Material Test System was used for the experiments. The diameter of the cylindrical punch and the supports is 10 mm. The total length L_1 and the span length L_0 of different arrangements depend on the ratio L_0/D and the diameter D of the outer profile. L_1

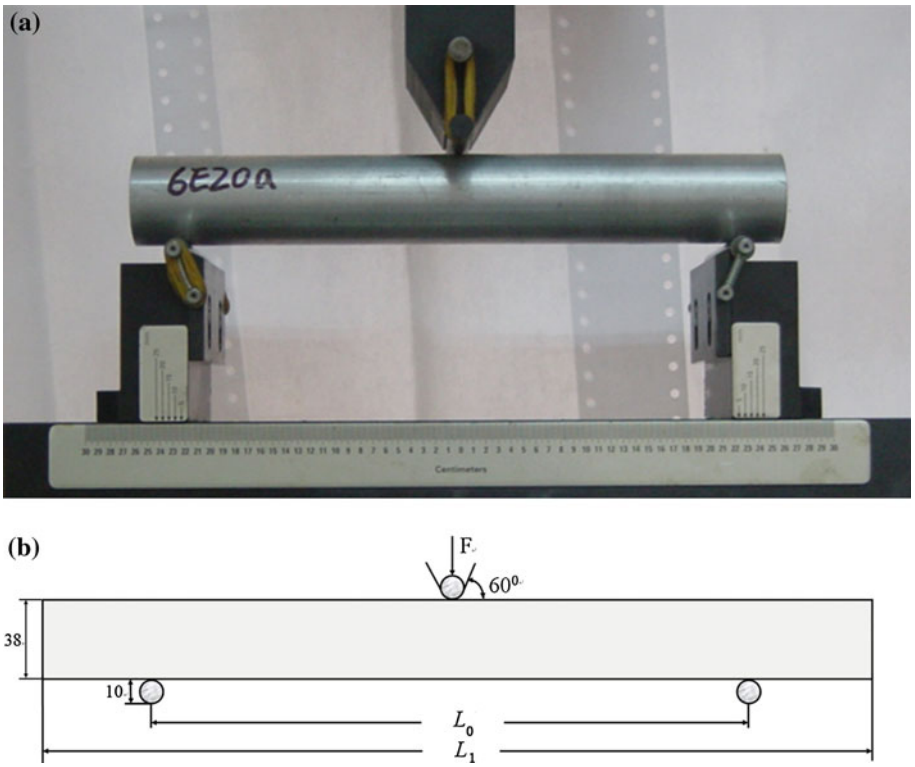

Fig. 4 **a** Test arrangement and **b** the dimensions of the experiments

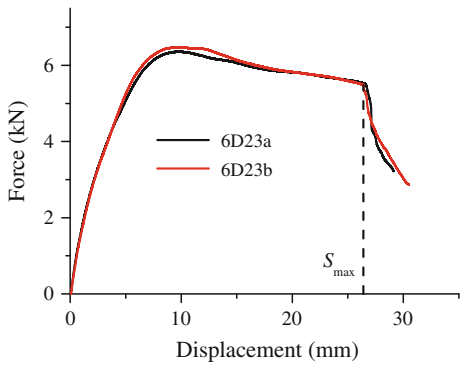

Fig. 5 The reproducibility of experiments

is 270 mm when L_0/D equals 6, and 190 mm when L_0/D equals 4. The angle between two wedged sides of the upper punch is about 60 degrees. A constant loading velocity of 0.2 mm/s was used to bend the specimens.

2.3 Definitions

In order to make a comparison of the experiment results easier, the following definitions are used in the paper.

$E = \int_0^S F\,\mathrm{d}s$ denotes the energy absorbed by the structure up to the displacement of S. When the maximum displacement $S_{\max}$ at global failure is chosen, the associated $E_{\max}$ represents the total energy the structure can absorb before failure. Here, the maximum displacement $S_{\max}$ is defined as the displacement when the force of the structure falls sharply at the late stage as the vertical dash line shown in Fig. 5.

$E_s = E/m_t$ denotes the specific energy absorption to describe the mass efficiency of the structure, where m_t is the total mass of a specimen. Again, when $E_{\max}$ is used as E, then E_{smax} represents the specific energy absorption of the structure before failure.

L_0/D=4

L_0/D=6

Fig. 6 Final deformation of different tube structures

3 Experimental results and discussion

3.1 Reproducibility of experiments

The force–displacement curves of two foam-filled double-tube specimens 6D23 are shown in Fig. 5. The reproducibility of other tests is also very good. Since the experiments are reproducible, only one curve for each structure is used in the comparison later.

3.2 Deformation and failure mode

Each test was finished either when the deflection reaches its maximum allowed by the test arrangement or when a crack was found. The final deformation of different structures is shown in Fig. 6. Apparently, the main differences in the deformation patterns of these structures are the indentation depth and the maximum deflection.

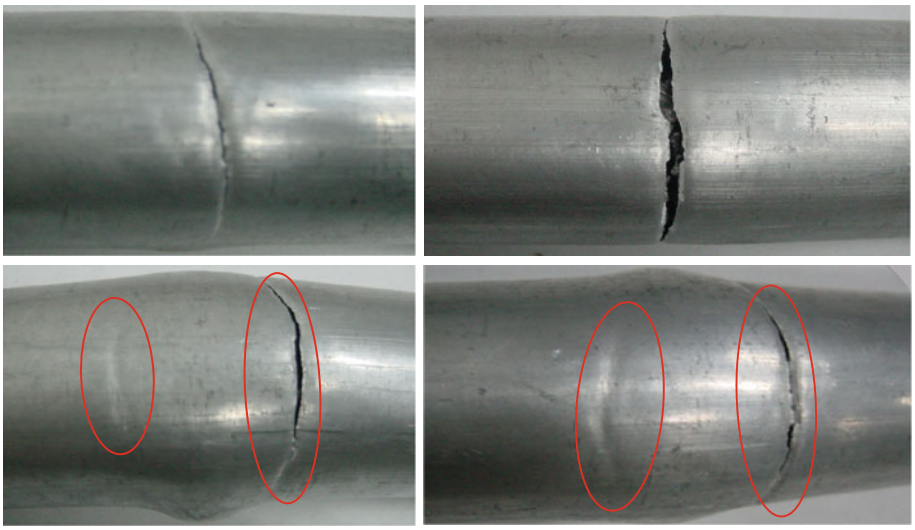

Fig. 7 Cracks and neckings in foam-filled single tubes (*upper*) and foam-filled double tubes (*lower*)

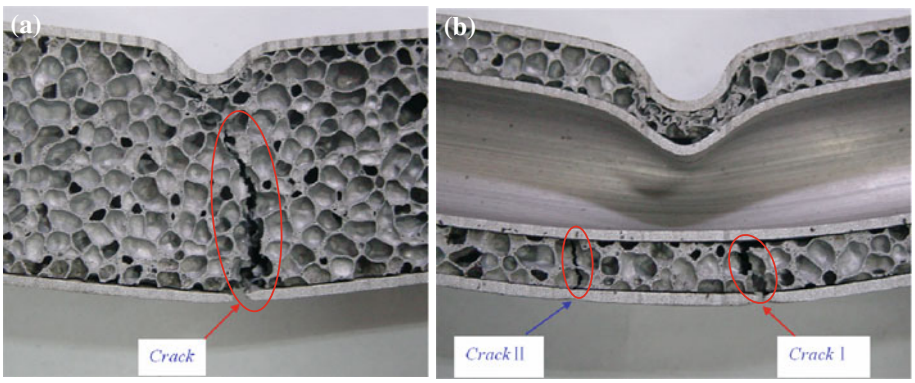

Fig. 8 Longitudinal sections of **a** a foam-filled single tube and **b** a foam-filled double tube

Comparing with foam-filled structures, the indentation of the empty tube is much more obvious and the final deflection is the largest. On the other hand, comparing with the foam-filled double-tube structure, the fold size of the foam-filled single tube is smaller but its final deflection is much smaller.

A more important feature of the results is that the failure modes of these structures are totally different. While no crack was found in the empty tube, both of the two foam-filled structures cracked at the downside. Comparisons between the two structures are shown in Figs. 7 and 8, showing the position of cracks and the sections of the fractured part, respectively. It can be seen that there is only one crack in the foam-filled single tube, which is just underneath the loading point. However, there are two cracks inside the foam of the double-tube structure, which are located symmetrically on the two sides, as shown in Fig. 8. Although only one crack can be found on the tube surface, a necking band located on the opposite side is obvious, as shown in Fig. 7. This is evidence that the cracks inside the foam occur earlier and lead to subsequent cracks in the outer tube. The mechanism will be discussed later in the numerical simulation.

3.3 Load-carrying capacity

The punch force–displacement curves for different structures are shown in Fig. 9. It should be noted that a rising of force in the late stage in specimen 4E20b is because the specimen surface comes into contact with the wedged sides of the upper punch at large rotation, and a sharp final drop of force in some specimens is associated with the fracture of the specimen.

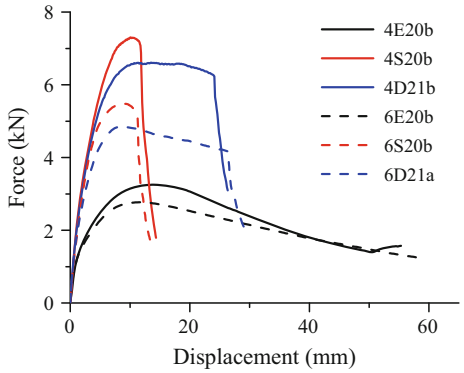

Fig. 9 Force–displacement curves of different tube structures

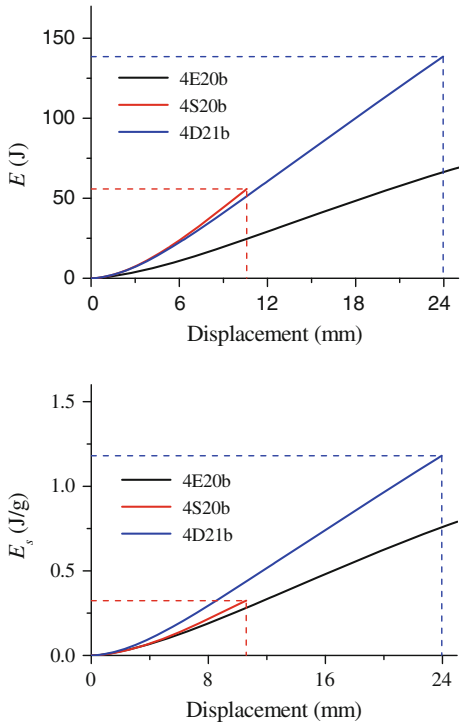

Fig. 10 Energy absorption of different structures

It can be seen from Fig. 9 that foam fillers increase the load-carrying capacity significantly. Another feature is the dropping trend of the force after its peak for the empty tube because of its serious indentation. The load-carrying capacity of the foam-filled single tube is the highest but it fails much earlier. Comparatively, the load-carrying capacity of the foam-filled double-tube structure is almost constant before failure, and the maximum displacement S_{max} is much larger than that of the foam-filled single tube, though its load-carrying capacity is slightly lower.

3.4 Energy absorption

The variations of energy absorption E and the specific energy absorption E_s with punch displacement for different structures having the same outer tube are shown in Fig. 10. The vertical and horizontal dash lines at the ends of the curves in this Figure denote the maximum displacement S_{max} of the punch and the energy absorption E_{max} or E_{smax} of the structure before failure, respectively. As expected, the energy absorption E of foam-filled structures is always much higher than that of empty tubes. Although the energy absorption E of

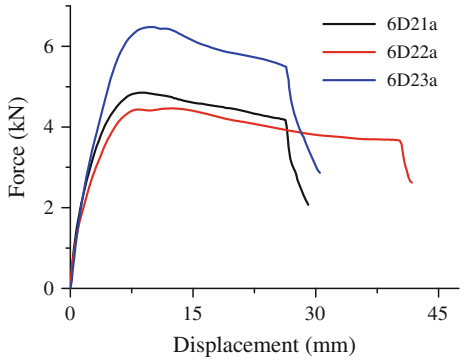

Fig. 11 Punch force–displacement curves of foam-filled double-tube structures with different inner tubes

a foam-filled single tube is a little bit higher than that of the foam-filled double-tube structure, the total energy absorption $E_{\max}$ of the latter is much higher than that of the former because of its large displacement before failure ($S_{\max}$).

From Fig. 10b, it can also be seen that the specific energy absorption E_s and $E_{s\max}$ of the foam-filled double-tube structure is much higher than that of the foam-filled single tube and the empty tube. In other words, foam-filled double tubes are more weight efficient than the other structures in energy absorption.

3.5 Effect of the span

A comparison of the punch force–displacement curves for different structures with different span is also shown in Fig. 9. It can be seen that the load-carrying capacity of all structures drops when L_0/D increases from 4 to 6. While the maximum displacement of the foam-filled double-tube structure becomes slightly larger, the load decreases faster after its peak.

3.6 Effect of the inner tube diameter and thickness

The punch force–displacement curves of foam-filled double-tube structures with different inner tubes are compared in Fig. 11. It is found that the force of specimen 6D22a with an inner tube diameter of 24 mm is only slightly lower than that of specimen 6D21a with a smaller inner tube diameter of 20 mm but the same thickness of 1.2 mm. However, its maximum displacement becomes significantly larger. Comparatively, when increasing both the inner tube diameter and thickness, specimen 6D23a with an inner tube diameter of 22 mm and thickness of 1.4 mm, the load-carrying capacity rises obviously but the maximum displacement is almost the same.

So, enlarging the inner tube increases the maximum displacement, and thickening the inner tube increases the load-carrying capacity but may reduce the maximum displacement.

3.7 Effect of the outer tube thickness

The effect of the outer tube thickness is shown in Fig. 12. It can be seen that thickening the outer tube increases both the load-carrying capacity and the maximum displacement and, as a result, the capacity of energy absorption. Particularly, if the outer tube is thick enough, e.g., 6D31 with the thickness 2.0 mm, the force decreases very slowly at the later stage. This behavior is of advantage for crashworthiness.

4 Numerical simulation

In order to explore the deformation and failure mechanism of the foam-filled double-tube structures, numerical simulations were conducted. The foam-filled single tubes were also studied for comparison.

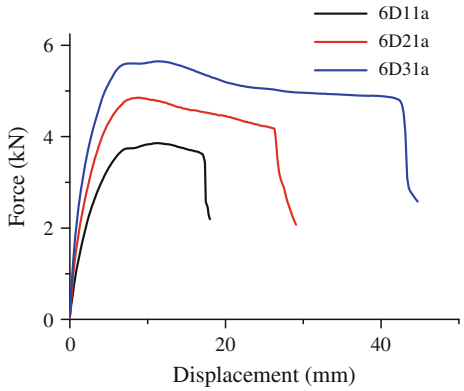

Fig. 12 Effect of the outer tube thickness

Table 3 The material parameters in detail

	ρ (g/cm^3)	E (GPa)	ν	ν_p	k
Tube	2.7	59	0.3		
Foam	0.43	0.625	0.1	0	1.732

4.1 Model

The explicit finite element code ABAQUS was used in the simulation. Three-dimensional models have been constructed, and nominal dimensions were used for the geometry, refer to Fig. 4b and Table 1. An elastic-plastic model was adopted to the aluminum alloy. The material model used in the simulation for the closed-cell aluminum foam is the crushable foam developed originally by Deshpande and Fleck [13]. The material parameters used in the simulations are obtained from the experiments and detailed in Table 3.

Considering the computational efficiency, the velocity of the upper punch was set as 10 mm/s in the simulation, faster than that actually used in the experiments. Nevertheless, its influence due to the inertia effect is negligible. The boundary conditions are the same as those in experiments.

A friction factor of 0.3 was set for the interface between the tube and foam, as well as for the self-contact of the tube. The interfaces between the outer profile and the upper punch or supports are keeping in contact. Shell and continuum solid elements were used for the tubes and foam, respectively, and a mesh size of 2 mm was used according to the mesh convergence analysis.

4.2 The force–displacement curves

Comparisons of the force–displacement curves of the two structures obtained experimentally and predicted numerically are shown in Fig. 13. Good agreement is reached except at a late stage after failure, since no fracture mechanism was incorporated in the simulation. It should be noted that a small number of foam cells appears along the thickness direction of the foam-filled double-tube structure, and the stress state shows a strong gradient in the foam layer. This may result in diverse of its average response from that of a block material due to the non-uniformity of the foam. So, the Deshpande–Fleck model is actually not applicable in this case. However, the overall response of the structure depends on both the property of the foam filler and that of the tubes. In the present case, the latter may be more important since the tubes bear most part of the bending load. The reduced influence and the randomness may, more or less, explain the agreement reached.

4.3 Tensile strain of the outer tube

The evolution of the maximum tensile strain at the lowest part of the outer tube in the foam-filled structures 6S20 and 6D21 is shown in Fig. 14. As the displacement of the punch U_u increases, the maximum tensile strain ε_m of the foam-filled double tube increases much slower than that of foam-filled single tube. This is in accordance with the deformation discussed in the previous Section. In other words, reaching the same tensile

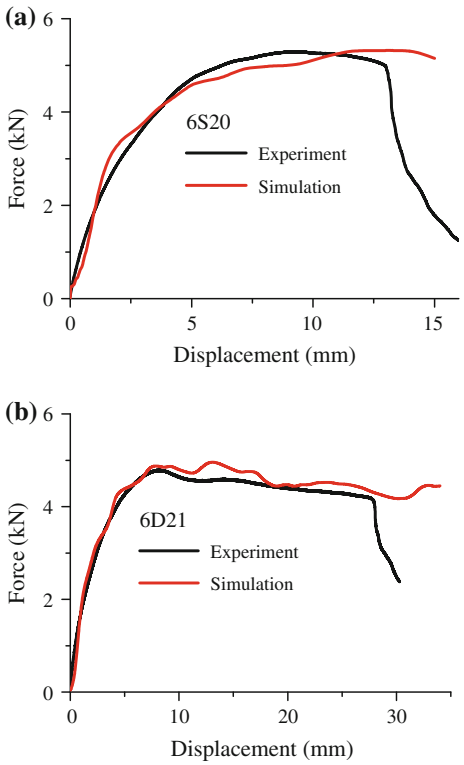

Fig. 13 Comparisons of the experimental and numerical results for **a** foam-filled single-tube and **b** foam-filled double-tube structures

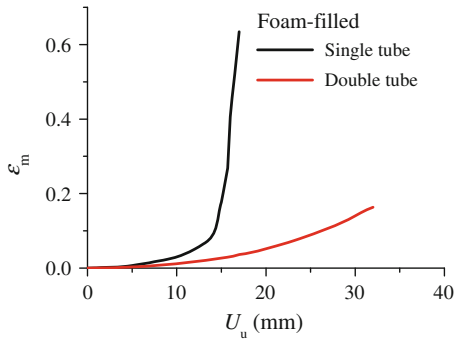

Fig. 14 Comparison of maximum strain evolution in foam-filled single-tube 6S20 and double-tube structures 6D21

strain, the deflection of the foam-filled double tube is larger than that of the foam-filled single tube, in agreement with the experimental results. So, the total energy absorption of the foam-filled double-tube structures before failure is enhanced, in comparison with the traditional foam-filled single tube.

4.4 Stress distribution and failure mechanism

In our experiments, there are two cracks located symmetrically about the center of the foam inside and happened before failure of the outer tube. In order to make the failure mechanism clear, we must investigate the stress distribution along the bottom path (dashed line) in the foam of the foam-filled double-tube structure shown in Fig. 15. From the results of our numerical simulation, we found that the hydrostatic stress distribution in the foam was similar to that in the foam-filled single tube. On the other hand, Fig. 16a shows that there are two peaks of the equivalent Mises stress located symmetrically about the center of the structure. Here, the horizontal coordinate zero locates the span center of the structure. The components of the deviatoric stress

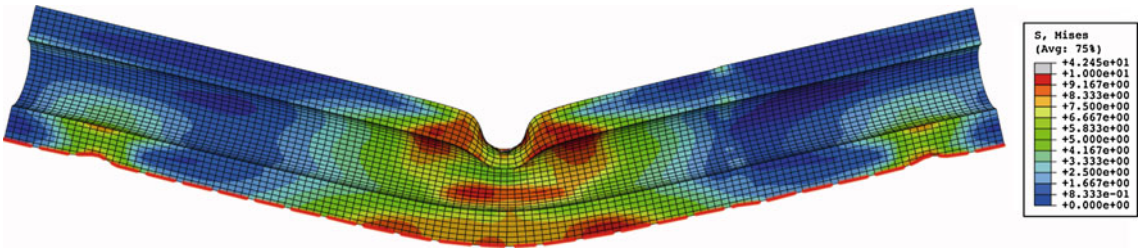

Fig. 15 Deformation and equivalent Mises stress distribution in the foam of sample 6D21

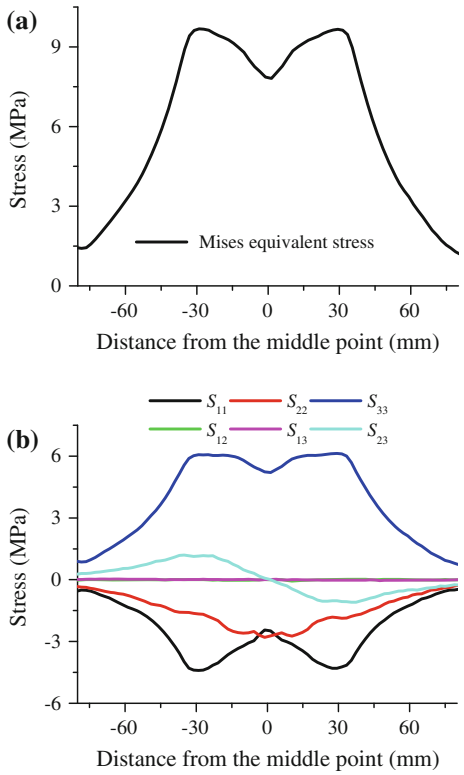

Fig. 16 Distributions of **a** Mises equivalent stress and **b** deviatoric stresses along the lowest part of foam in sample 6D21

tensor are shown in Fig. 16b. The deviatoric shear stresses are almost zero except S_{23}. Both S_{11} (circumferential direction) and S_{33} (axial direction) also have two peaks, and the distance between the two peaks is almost equal to the distance between the two cracks in the foam observed experimentally. These evidences explain the failure mechanism of the foam-filled double-tube structure, though a reliable failure criterion is not available yet. This trend presented also suggests that improving the tensile strength of the foam may further enhance the energy absorption capacity of the foam-filled double-tube structure.

4.5 Conclusions and discussions

In this paper, the quasi-static three-point bending behavior of foam-filled double-tube structures is studied by experiments and finite element simulations, and the results are compared with those of empty tubes and traditional foam-filled single tubes. Experimental results show that the foam-filled double-tube structure can carry a steady load with enhanced bending resistance, higher energy absorption capacity, and weight efficiency.

Both experimental investigation and numerical simulations reveal that the deformation and failure mechanism of the new structure are different from those of an empty tube and foam-filled single tube. The tensile strain along the bottom of the outer tube increases slower, and the failure of the outer tube at the bottom-center was delayed. Two cracks located symmetrically on both sides at a distance from the loading position were

found experimentally. Observation of the specimen section shows that cracks initiated in the aluminum foam. The stress distributions calculated by the FE method approve this failure mechanism.

In this paper, we focus our attention on the effect of the structural topology and a few structural parameters. In our early study [7], we have found that foam density may affect the bending and failure behavior of the structure. However, only a limited range of the foam density was used in the present study. More experiments should be conducted to investigate the influence of foam density and other parameters.

As mentioned in Refs. [6,8], partial foam filling can significantly increase the specific energy absorption of foam-filled single tubes. It would be expected that partial filling could increase the specific energy absorption of foam-filled double tubes as well, though it should be approved in the future.

Acknowledgments This work is supported by the National Natural Science Foundation of China (projects numbers 90916026, 90205003, 10532020, and 10672156).

References

1. Wierzbicki, T., Abramowicz, W.: On the crushing mechanics of thin-walled structures. J. Appl. Mech. **50**, 727–739 (1983)
2. Abramowicz, W., Wierzbicki, T.: Axial crushing of foam-filled columns. Int. J. Mech. Sci. **30**, 263–271 (1988)
3. Seitzberger, M., Rammerstorfer, F., Gradinger, R., Degischer, H., Blaimschein, M., Walch, C.: Experimental studies on the quasi-static axial crushing of steel columns filled with aluminum foam. Int. J. Solids Struct. **37**, 4125–4147 (2000)
4. Kallina, I., Zeidler, F., Baumann, K., Scheunest, D.: The offset crash against a deformable barrier, a more realistic frontal impact. In: Proceedings of the 14th International Technical Conference on Enhanced Safety of Vehicles, vol. 2, pp. 1300–1304. Munich, Germany (1994)
5. Santosa, S., Wierzbicki, T.: Effect of an ultralight metal filler on the bending collapse behavior of thin-walled prismatic columns. Int. J. Mech. Sci. **41**, 995–1019 (1999)
6. Santosa, S., Banhart, J., Wierzbicki, J.: Experimental and numerical analyses of bending of foam-filled sections. Acta Mech. **148**, 199–213 (2001)
7. Xie, Z.Y., Yu, J.L., Li, J.R.: An experimental study on three-point bending of aluminum alloy foam-filled cylindrical aluminum alloy pipe. J. Exp. Mech. **22**, 104–110 (2007). (in Chinese)
8. Xie, Z.Y., Li, J.R., Yu, J.L.: Numerical simulation of three-point bending experiments of thin-walled cylindrical tubes filled with aluminum foam. Acta Mech. Solida Sin. **28**, 261–265 (2007). (in Chinese)
9. Chen, W.: Experimental and numerical study on bending collapse of aluminum foam-filled hat profiles. Int. J. Solids Struct. **38**, 7919–7944 (2001)
10. Chen, W., Wierzbicki, T., Santosa, S.: Bending collapse of thin-walled beams with ultralight filler: numerical simulation and weight optimization. Acta Mech. **153**, 183–206 (2002)
11. Zarei, H.R., Kröger, M.: Bending behavior of empty and foam-filled beams: structural optimization. Int. J. Impact Eng. **35**, 521–529 (2008)
12. Kim, A., Cheon, S.S., Hasan, M.A., Cho, S.S.: Bending behavior of thin-walled cylindrical tube filled with aluminum alloy foam. Key Eng. Mater. **270–273**, 46–51 (2004)
13. Deshpande, V.S., Fleck, N.A.: Isotropic constitutive model for metallic foams. J. Mech. Phys. Solids **48**, 1253–1276 (2000)